Value of digital mammography in predicting lymphovascular invasion of breast cancer

Zhuangsheng Liu
Jiangmen Central Hospital
Xiaoping Li
Jiangmen Central Hospital
Keming Liang
Jiangmen Central Hospital
Junhao Chen
Jiangmen Central Hospital
Xiangmeng Chen
Jiangmen Central Hospital
Ruqiong Li
Jiangmen Central Hospital
Ronggang Li
Jiangmen Central Hospital
Xin Zhang
Jiangmen Central Hospital
Lilei Yi
Foshan Hospital of Traditional Chinese Medicine
Wansheng Long (jmlws2@163.com)
Jiangmen Central Hospital https://orcid.org/0000-0002-1331-1858

Research article

Keywords: Lymphovascular invasion, Breast, Cancer, Digital mammography

Posted Date: December 16th, 2019

DOI: https://doi.org/10.21203/rs.2.18849/v1

Abstract

Background: To use digital mammography, a more popular imaging tool, for predicting lymphovascular invasion(LVI) in breast cancer patients preoperatively.

Methods: 122 cases of invasive ductal carcinoma diagnosed between May 2017 and September 2018 were collected, which were divided into positive group (n=42) and negative group (n=80) according to the presence or absence of LVI.

Results: The differences of these variables(childbearing history, miscarriage history, other breast diseases history, nipple discharge, breast cancer marker CA153, age, ER, PR, HER-2, E-CAD, P53, Ki-67) between LVI positive group and the LVI negative group were not statistically significant, except that of Ki-67 (P=0.012). For the image features of digital mammography, the differences of interstitial edema (P=0.013) and skin thickening (P=0.000) between LVI positive group and negative groups were statistically significant. The differences of other imaging patterns, that is, fibroglandular tissue density, size , solitary/multiple, mass shape, mass margin , subcutaneous fat, axillary adenopathy and so on, between the two groups were not statistically significant. Multiple factor analysis shows that, there are three independent risk factors for predicting LVI occurrence: interstitial edema (OR = 12.610, 95% confidence interval CI: 1.061, 149.922, P=0.045), subcutaneous fat (OR=0.081, 95% confidence interval CI: 0.012, 0.645, P =0.017) and skin thickening (OR=9.041, 95% confidence interval CI: 2.553, 32.022, P=0.001).

Conclusion: Interstitial edema, blurring of subcutaneous fat layer, and skin thickening were independent risk factors for predicting LVI occurrence. When applying these three imaging patterns together, the specificity of LVI prediction was as high as 98.8%.

1. Background

Breast cancer metastasizes through lymphatic and blood vessels, which makes it a major factor for distant metastasis, postoperative recurrence and even death [1]. Lymphovascular invasion (LVI) is never revealed by preoperative imaging scans. Diagnostic histopathology is needed to reveal lymphovascular invasion of cancer cells. Identification of lymphovascular invasion preoperatively can help predict prognosis of patients with breast cancer, especially those with axillary node-negative breast cancer, and develop adjuvant treatment plans in clinical settings [2, 3]. Therefore, preoperative prediction of lymphovascular invasion with imaging devices is of great clinical value.

Digital mammography is one of the important imaging tools for breast cancer screening and diagnosis. THERE ARE MANY REPORTS ON THE PREDICTION OF AXILLARY LYMPH NODE METASTASIS[4–6], DIGITAL MAMMOGRAPHY SCREENING[7–10]. However, no study reports on predicting lymphovascular invasion in breast cancer patients based on imaging patterns of digital mammography have been found, except A FEW LITERATURE REPORTED that [3, 11–13] predicts lymphovascular invasion in breast cancer patients using MRI findings.

It is necessary to use digital mammography, a more popular imaging tool, for predicting lymphovascular invasion in breast cancer patients preoperatively, and evaluate its findings in combination with certain biomarkers detected by immunohistochemistry to better foresee the disease progression and develop targeted treatment plan.

2. Methods

2.1 Clinical data

This is a single-center retrospective study. All breast cancer cases were obtained from picture archiving and communication system(PACS), so patients' informed consent was not required. THIS RETROSPECTIVE STUDY WAS APPROVED BY OUR HOSPITAL'S ETHICS COMMITTEE. In all collected cases, mammographic lesions were confirmed either by core needle biopsies or by surgical pathology; and all patients underwent digital mammography preoperatively. In this study, 158 cases of invasive ductal carcinoma diagnosed between May 2017 and September 2018 were randomly selected. The inclusion criteria were: (1) patients underwent modified radical mastectomy or breast-conserving surgery + axillary lymph node dissection; (2) diagnosis of invasive breast cancer was confirmed by routine histopathological and immunohistochemical examinations ; (3) previous history of breast tumors and the primary tumors in other locations were excluded; (4) lymphovascular tumor emboli were detected by pathologists using immunohistochemistry. 122 cases were retained, after excluding those with obscure lesions presented by digital mammograms, breastfeeding patients, patients who had underwent lumbar puncture or radiotherapy prior to the diagnosis, and incomplete clinical data. In these eligible cases, all patients were female, aged between 26 and 77 years, with a median age of 45 years.

2.2 Digital mammography

GE (Senographe DS) and IMS (GIOTTO IMAGE) systems were used. Four standard body positions, right craniocaudal(RCC), left craniocaudal(LCC), right mediolateral oblique(RMLO) and left mediolateral oblique(LMLO) were adopted under at automatic exposure conditions. When lesions were found in the axillary tail of Spence and near the cleavage, amplified imaging in these locations was added to fully reveal the lesions. The internal and external oblique flat-panel detector was parallel to the pectoralis major muscle. According to patients' body shape, the projecting angle ranged from 40 ° to 65 °, and was usually at 60 °. The glands were fully unfolded, and the skin folds under the breasts and upper abdomen were within the mammographic field.

2.3 Image analysis

The imaging characteristics of breast cancer lesions were described according to the 5th edition of ACR BI-RADS-X Atlas published in 2013 (breast imaging-reporting and data system) [14]. The lesions are classified into masses, calcifications, architectural distortion, and asymmetries. The masses can be solitary or multiple, and their shapes are described as round, lobulated, and irregular. Margins of the masses can be described as well circumscribed if they have clear and sharp edges. Also, the margins can

be described as obscured if the viewer believes they have clear and sharp edges which are obscured by glands. Margins are described as instinct if they have obscure and speculated edges. In this study group, amorphous and fine polymorphic calcifications were included while excluding typically benign calcification. Architectural distortion is defined as the abnormal deformation of the breast, without being revealed by any clear mass. In such case, history of trauma and surgery must be ruled out. A focal asymmetry is seen in two images, but lacks the outward border or a mass. In this study group, only few cases of architectural distortion and focal asymmetry (both $n < 5$) on digital mammography were found. Therefore, these cases were ruled out from study samples to avoid inaccuracy of statistical results. And the lesion type was classified as mass and calcification only.

The locations of lesion are divided into the upper outer quadrant, the lower outer quadrant, the lower inner quadrant, the upper inner quadrant, the central region and the whole breast. The breast composition were described as: a. almost entirely fatty; b. there are scattered areas of fibroglandular density; c. heterogeneously dense, which may obscure small masses; and d. extremely dense, which lowers the sensitivity of mammography. Associated features included interstitial edema, blurring of subcutaneous fat layer, skin thickening, and axillary adenopathy (lymph nodes measuring > 1 cm in the long axis diameter with absence of hilus).

2.4 Pathology

Surgically resected breast cancer specimens were fixed in 10% formaldehyde for 24 h, then were dehydrated and embedded in paraffin wax. Sections were prepared. Standard HE staining and streptavidin-peroxidase-biotin (SP) immunohistochemical method were performed. A DAB detection system were performed. Her-2 scoring 3 + was defined as overexpression. For Her-2 scoring 2+, the Her-2 gene amplification was tested by FISH, whose positive result would be defined as overexpression. Ki67 proliferative index (PI) was scored as low expression when < 10%, high expression when > 30%, and intermediate expression when it was between 10% and 30% [15].

The gold standard of this study: lymphovascular invasion is defined as the intravenous tumor emboli and lymphatic tumor emboli detected by immunohistochemistry. These two kinds of tumor emboli were clinically referred to as intralymphovascular tumor emboli due to the difficulty of distinguishing them by pathological sections. The speciments were read by a senior pathologist who has been working on breast cancer for 21 years.

2.5 Statistical analysis

The cases were classified into lymphovascular invasion positive group (LVI positive group) and lymphovascular invasion negative group (LVI negative group), according to the clinical and imaging characteristics of invasive ductal carcinoma. Table 1–3 was completed. The data were analyzed using SPSS Version 19.0 statistical package. The quantitative data was expressed by ± sd. The Independent Two-sample t Test were used for comparison between groups; the count data was expressed by frequency or rate, and the $\chi 2$ test or Fisher's method was used, with $P < 0.05$ indicating that the difference is statistically significant. All count data with 0 s were excluded in statistical analysis, and was listed

only. The Nomogram was used to analyze the risk factors of LVI occurrence. The two-tailed was performed with $P < 0.05$ being considered as statistically significant.

3. Results

3.1 General data and biomarkers

122 breast IDC patients were divided into positive group (n=42) and negative group (n=80) according to the presence or absence of lymphovascular invasion . The classification results of childbearing history, miscarriage history, other breast diseases history, nipple discharge, breast cancer marker CA153, age, ER, PR, HER-2, E-CAD, P53, Ki-67 are shown in Table 1. Due to the absence of nipple discharge (n=0) in the LVI negative group, the nipple-discharge variable was excluded, and was listed only. The differences of the variables between LVI positive group and the LVI negative group were not statistically significant, except that of Ki-67 (P=0.012).

3.2 The image patternsof digital mammography

Details are shown in Table 1. The differences of interstitial edema (P=0.013, Fig.1, 2) and skin thickening (P=0.000,Fig. 1,2) between LVI positive group and negative groups were statistically significant. The differences of other imaging patterns, that is, fibroglandular tissue density (P=0.431), size (P=0.094), solitary/multiple (P=0.746), lesions (P=0.8855), location (P=0.879), mass shape (P=0.160), mass margin (P=0.088), boundary (P=0.714), calcification (P=0.279), subcutaneous fat (P=0.697), nipple retraction (P=0.073), axillary adenopathy (P =0.166), between the two groups were not statistically significant.

Risk factor analysis: See Table 2. Multiple factor analysis (MFA) shows that, there are three independent risk factors for predicting LVI occurrence: interstitial edema (OR = 12.610, 95% confidence interval CI: 1.061, 149.922, P=0.045), subcutaneous fat (OR=0.081, 95% confidence interval CI: 0.012, 0.645, P =0.017) and skin thickening (OR=9.041, 95% confidence interval CI: 2.553, 32.022, P=0.001).

Table 3 shows the sensitivity, specificity, accuracy, PPV and NPV of the above three imaging patterns with LVI predicting values: interstitial edema, subcutaneous fat and skin thickening, and their combined application in LVI predictions. The specificity of LVI prediction was as high as 98.8% when these three imaging patterns were applied together.

4. Discussion

lymphovascular invasion (intralymphovascular tumor emboli) is closely related to the adverse outcome of many malignant tumors [16–18]. As a risk factor for recurrent breast cancer following modified radical mastectomy, lymphovascular tumor emboli, especially lymphatic tumor emboli, has been included in the St Gallen consensus for breast cancer [19]. Karlsson et al's [20] study results showed that the failure rate of chemotherapy in breast cancer patients detected with lymphovascular invasion was higher. Shen et al [21] showed that lymphovascular tumor emboli can promote local tumor recurrence and distant metastasis. Therefore, lymphovascular tumor emboli is a reliable indicator for the distant metastasis of

breast cancer and the assessment of patients' overall survival. We intended to predict the risk of lymphovascular invasion of the most common invasive ductal carcinoma using various imaging patterns of digital mammography, the most commonly used imaging tool.

From the data of this study group, there was no statistical significance of the differences in the age, childbearing history, miscarriage history, family history and other medical history between the LVI positive group and the LVI negative group. Nulliparity, miscarriage, and family history of breast cancer do not increase the LVI occurrence rate in breast cancer patients. First discovered in breast cancer and breast cells, CA153 is a tumor marker with relatively higher specificity for breast cancer diagnosis. With the advancing of breast cancer, the CA153 sensitivity increased from 66–80% [22]. However, in this study group, there were only 4 (3.3%) CA153 positive cases. While no statistical significance was found in differences of ER, PR, Her-2, E-cad, and P53 between the LVI positive group and the LVI negative group, cases with high expression of Ki-67 (> 30%) in the LVI positive group were more than that in the LVI negative group, which was statistically significant (P = 0.012). Many literatures have also confirmed that Ki-67 is associated with tumor differentiation, lymphovascular invasion, metastasis, and recurrence [23–25].

The data of this study group showed that there is no difference in mammographic background presented by digital mammography and direct patterns of breast cancer, such as mammographic density, location of mass, number, size, shape, margin, boundary, calcification classification, etc., between LVI positive group and LVI negative group. Therefore, the above imaging patterns cannot be used to predict LVI occurrence. Also, heterogeneously dense and extremely dense breast do not increase the risk of LVI occurrence. However, the differences in indirect features such as interstitial edema and breast skin thickening between LVI positive group and LVI negative group were statistically significant (P = 0.013 and 0.000, respectively). In addition, multivariate analysis indicated that interstitial edema, blurring of subcutaneous fat layer, and skin thickening were independent risk factors for predicting LVI occurrence (P = 0.045, 0.017 and 0.001, respectively). In clinical work-up, physicians should be highly vigilant about LVI occurrence once the above three imaging patterns are found on digital mammography. Even if lymph node metastasis is negative in sentinel lymph node and axillary lymph node biopsies, possibility that breast cancer cells has infiltrated into surrounding vessels but not yet reached upwards to the axillary lymph nodes should be considered. Accordingly, adjustments in postoperative adjuvant therapy should be considered to reduce risk of recurrence and distant metastasis and thus improve patients' survival time.

We have thought that the axillary lymph nodes shown on digital mammography could be used to predict LVI occurrence. However, this group of study data shows that there is no difference in the size and shape of axillary lymph nodes between the LVI positive group and the LVI negative group (P = 0.166), which might be explained by failure of displaying axillary lymph nodes on the digital mammography image. In addition, lymph node enlargement (> 1 cm) and a full shape does not always mean lymph node metastasis, it may also suggest lymphoid node reactive hyperplasia.

Nomogram is a statistical model used for individualized predictive analysis of clinical events. Compared with other predictive statistical methods, Nomogram analysis provides a better individualized prognostic risk assessment in an intuitive, visual way [26]. This study also established a nomogram model for predicting the risk of LVI occurrence in individuals based on digital mammographic imaging patterns. For example, we can learn from Fig. 3 that, if the patient presents with interstitial edema, subcutaneous fat, and skin thickening, along with Ki-67 high expression, the score will be 95 + 100 + 87 + 48 = 330 points, with the corresponding risk of LVI being 68%. In this way, clinicians can better understand patients' clinical prognosis, and develop a more effective and targeted therapeutic regime.

5. Conclusions

There was a statistically significant difference in Ki-67 between the LVI positive group and the LVI negative group. Interstitial edema, blurring of subcutaneous fat layer, and skin thickening were independent risk factors for predicting LVI occurrence (P = 0.045, 0.017, and 0.001, respectively). When applying these three imaging patterns together, the specificity of LVI prediction was as high as 98.8%.

Declarations

Ethics approval and consent to participate

The Ethics Committee of the Affiliated Jiangmen Hospital of Sun Yat-Sen University approved the current study, and the need for signed informed consent was waived.

Consent for publication

Not applicable.

Availability of data and materials

The data needed to replicate the current findings are available in the figures and tables of the main article. Because of patient privacy protection, additional study materials are only available upon individual request directed to the corresponding author.

Competing interests

The authors declare that they have no conflicts of interest regarding the publication of this paper.

Funding

This work was supported by the National Natural Science Foundation of China (81802918), the science and technology planning project of Jiangmen (2017A4016), and the science and technology planning project of Jiangmen(2015068). These funding are earmarked for cancer research. The funding bodies have no role in study design, collection, analysis, interpretation of data or writing the manuscript.

Author contributions

ZSL, RQL participated in the study design, evaluated the results and wrote the first and revised manuscript. KML, JHC and XMC participated in the study design and supplied with contrast medium. XPL RGL and XZ carried out the images analysis and revised manuscripts. LLY, WSL participated in the design of the study, redesigned the data analysis. All authors read and approved the final manuscript.

Acknowledgment

We thank the study team at Jiangmen Central Hospital for their continuous support.

Abbreviations

LVI: lymphovascular invasion DM: digital mammography DBT: digital breast tomosynthesis CESM: contrast-enhanced digital mammography PACS: picture archiving and communication system RCC : right craniocaudal LCC: left craniocaudal RMLO: right mediolateral oblique LMLO : left mediolateral oblique

References

1. W. Wang, A. Belosay, X. Yang, J.A. Hartman, H. et al. Effects of letrozole on breast cancer micro-metastatic tumor growth in bone and lung in mice inoculated with murine 4T1 cells. Clin Exp Metastasis. 2016;33(5):475-85
2. A. Rezaianzadeh, A. Talei, A. Rajaeefard, et al.lymphovascular invasion as an independent prognostic factor in lymph node negative invasive breast cancer. Asian Pac J Cancer Prev. 2012;13(11):5767-72.
3. Fs Oy,Bl G,Xy H, et al. A nomogram for individual prediction of lymphovascular invasion in primary breast cancer. Eur J Radiol. 2019 Jan;110:30-38.
4. JB Yang, T Wang, LF Yang,et al. Preoperative Prediction of Axillary Lymph Node Metastasis in Breast Cancer Using Mammography-Based Radiomics Method. Sci Rep. 2019; 9: 4429.
5. DZ Cen, L Xu, SW Zhang,et al. BI-RADS 3–5 microcalcifications: prediction of lymph node metastasis of breast cancer. Oncotarget. 2017 May 2; 8(18): 30190–30198.
6. Önder Karahallı, Turan Acar, Murat Kemal Atahan, et al. Clinical and Pathological Factors Affecting the Sentinel Lymph Node Metastasis in Patients with Breast Cancer. Indian J Surg. 2017 Oct; 79(5): 418–422.

7. RA. Hubbard, Weiwei Zhu, Ruslan Horblyuk, et al. Diagnostic imaging and biopsy pathways following abnormal screen-film and digital screening mammography.Breast Cancer Res Treat. 2013; 138(3): 879–887.
8. Christoph I. Lee, Mucahit Cevik, Oguzhan Alagoz, et al. Comparative Effectiveness of Combined Digital Mammography and Tomosynthesis Screening for Women with Dense Breasts. Radiology. 2015; 274(3): 772–780.
9. Patricia I. Jewett, Ronald E. Gangnon, Elena Elkin, et al. Geographic access to mammography facilities and frequency of mammography screening. Ann Epidemiol. 2018; 28(2): 65–71.
10. Cristina O'Donoghue, Martin Eklund, Elissa M, et al. Aggregate Cost of Mammography Screening in the United States: Comparison of Current Practice and Advocated Guidelines.Ann Intern Med. 2014; 160(3): 145.
11. Hyejin C, Hye JK, So ML, et al. Preoperative MRI Features Associated With Lymphovascular Invasion in Node-Negative Invasive Breast Cancer: A Propensity-Matched Analysis. Journal of Magnetic Resonance Imaging. 2017;46 (4):1037-1044.
12. Mori N, Mugikura S, Takasawa C, et al. Peritumoral apparent diffusion coefficients for prediction of lymphovascular invasion in clinically node-negative invasive breast cancer. Eur Radiol 2016;26:331–339.
13. Liu ZS, Bao F, Li CL, et al. Preoperative Prediction of Lymphovascular Invasion in Invasive Breast Cancer With Dynamic Contrast-Enhanced-MRI-Based Radiomics. J Magn Reson Imaging.2019 Feb 17. [Epub ahead of print].
14. American College of Radiology(ACR). Breast imaging reporting and data system(BI-RADS). 5th ed. Reston,Va:Ameirican College of Radiology,2013.P133.
15. Violetta Barbashina , D Adriana. MD Corben. Mucinous micropapillary carcinoma of the breast:an aggressive counterpart to conventional pure mucinous tumors. Human Pathology 2013,44:1577-1585.
16. JW Liang , P Gao, ZN Wang ,et al. The integration of macroscopic tumor invasionof adjacent organs into TNM staging system for colorectal cancer. Plos One.2012.7(12):52269.
17. JH Lai, YJ Zhou, D Bin, et al. Clinical significance of detecting lymphatic and blood vessel invasion in stage II colon cancer using markers D2-40 and CD34 in combination. Asian Pac J Cancer Prev, 204, 15(3):1363-1367.
18. E Matloff . Cancer Principles and Practice of Oncology: Handbook of Clinical Cancer Genetics. J Am Med Associa. 1990,248(15):1904-1905.
19. MIgnatiadis , M Buyse, C Sotiriou. St Gallen International Expert Consensus on the primary therapy of early breast cancer: an invaluable tool for physicians, and scientists. Ann Oncl, 2012, 26(8): 1519-1520.
20. P Karlsson, BF Cole, KN Price, et al. The role of the number of uninvolved lymph nodes in predicting locoregional recurren in breast cancer. J Clin Oncol, 2007,25(15):2019-2026.

21. S Shen, S Zhong, Lu H, et al. A meta-analysis of lymphatic vessel invasion correlated with pathologic factors in invasive breast cancer. J Cancer Ther,2015,6:315-321.
22. JW Choi , BI Moon , JW Lee ,et al. Use of CA15-3 for screening breast cancer: An antibody-lectin sandwich assay for detecting glycosylation of CA15-3 in sera. Oncol Rep. 2018 Jul;40(1):145-154.
23. SS Menon , C Guruvayoorappan , KM Sakthivel , et al. Ki-67 protein as a tumour proliferation marker. Clin Chim Acta.2019 Jan 14;491:39-45.
24. H Zhang, X Sui, S Zhou, et al. About "Correlation of conventional ultrasound characteristics of breast tumors with axillary lymph node metastasis and ki-67 expression in patients with breast cancer". J Ultrasound Med. 2019 Jan 14. doi: 10.1002/jum.14930. [Epub ahead of print] .
25. JH Peng , X Zhang , JL Song, et al. Neoadjuvant chemotherapy reduces the expression rates of ER, PR, HER2, Ki67, and P53 of invasive ductal carcinoma. Medicine (Baltimore). 2019 Jan;98(2):e13554.
26. S Li , J Zhao , L Zhu , et al. Development and validation of a nomogram predicting the overall survival of stage IV breast cancer patients. Cancer Med.2017 Nov;6(11):2586-2594.

Tables

Table.1 Comparison of patient characteristics according to Vascular invasion

Characteristics	Total	VI=0(Negative)	VI=1(Positive)	P
Age	122	49.99(10.17)	48.93(9.34)	0.566
History of giving birth	122	80	42	0.488
No	5	4(5.00)	1(2.38)	
Yes	117	76(95.00)	41(97.62)	
History of abortion	122	80	42	0.560
No	86	55(68.75)	31(73.81)	
Yes	36	25(31.25)	11(26.19)	
nipple discharge	122	80	42	
No	120	80(100.00)	40(95.24)	
Yes	2	0(0.00)	2(4.76)	
CA153*	121	79	42	0.514
Negative	117	77(97.47)	40(95.24)	
Positive	4	2(2.53)	2(4.76)	
History of related illness	122	80	42	0.488
No	117	76(95.00)	41(97.62)	
Yes	5	4(5.00)	1(2.38)	
ER	122	80	42	0.062
Negative	39	21(26.25)	18(42.86)	
Positive	83	59(73.75)	24(57.14)	
PR	122	80	42	0.0591
Negative	47	26(32.50)	21(50.00)	
Positive	75	54(67.50)	21(50.00)	
HER-2	122	80	42	0.994
Negative	32	21(26.25)	11(26.19)	
Positive	90	59(73.75)	31(73.81)	
E-cad*	87	56	31	0.100
Negative	6	2(3.57)	4(12.90)	
Positive	81	54(96.43)	27(87.10)	
Ki-67	122	80	42	0.012
Low	27	20(25.00)	7(16.67)	
Moderate	36	29(36.25)	7(16.67)	
High	59	31(38.75)	28(66.67)	
P53	122	80	42	0.126
Negative	40	30(37.50)	10(23.81)	
Positive	82	50(62.50)	32(76.19)	
Amount of fibroglandular tissue	122	80	42	0.431
Almost entirely fat/Scattered fibroglandular tissue	49	33(41.25)	16(38.10)	
Heterogeneous fibroglandular tissue	54	37(46.25)	17(40.48)	
Extreme fibroglandular tissue	19	10(12.50)	9(21.43)	
Size(cm)	122	80	42	0.094
No	79	56(70.00)	23(54.76)	
Yes	43	24(30.00)	19(45.24)	
Single/multiple	122	80	42	0.746
Single	95	63(78.75)	32(76.19)	
Multiple	27	17(21.25)	10(23.81)	
Lesions	122	80	42	0.8855
Mass	65	43(53.75)	22(52.38)	
Mass/calcification	57	37(46.25)	20(47.62)	
Location	122	80	42	0.879
Outer upper	73	49(61.25)	24(57.14)	
Outer lower	5	4(5.00)	1(2.38)	
Lower inner	15	10(12.50)	5(11.90)	
Upper inner	15	9(11.25)	6(14.29)	
Central area	14	8(10.00)	6(14.29)	

Mass shape	122	80	42	0.160
Lobulated	16	8(10.00)	8(19.05)	
Irregular	106	72(90.00)	34(80.95)	
Mass Margin	122	80	42	0.088
Smooth	6	2(2.50)	4(9.52)	
Rough	116	78(97.50)	38(90.48)	
Boundary	122	80	42	0.714
Clear	69	47(58.75)	22(52.38)	
Obscure	27	16(20.00)	11(26.19)	
Shield	26	17(21.25)	9(21.43)	
Calcification*	56	36	20	0.279
Vague and amorphous	25	18(50.00)	7(35.00)	
Fine polymorphous	31	18(50.00)	13(65.00)	
Interstitial edema	122	80	42	0.013
No	110	76(95.00)	34(80.95)	
Yes	12	4(5.00)	8(19.05)	
Subcutaneous fat	122	80	42	0.697
Clear	101	67(83.75)	34(80.95)	
Muddy	21	13(16.25)	8(19.05)	
Thicken Skin	122	80	42	0.000
No	86	65(81.25)	21(50.00)	
Yes	36	15(18.75)	21(50.00)	
Nipple retraction	122	80	42	0.073
No	98	68(85.00)	30(71.43)	
Yes	24	12(15.00)	12(28.57)	
Axillary lymph node enlargement	122	80	42	0.166
No	77	54(67.50)	23(54.76)	
Yes	45	26(32.50)	19(45.24)	

* Missing value exists

VI：Vascular invasion

Table 2. Univariate and multivariate analysis

Factors	Univariate analysis		Multivariate analysis	
	OR（95%*CI*）	*P*	*OR*（95%*CI*）	*P*
Interstitial edema	4.471(1.260,15.864)	**0.020**	**12.610(1.061,149.922)**	**0.045**
Subcutaneous fat	1.213(0.458,3.207)	0.698	**0.081(0.012,0.645)**	**0.017**
Thicken Skin	4.333(1.899,9.891)	**0.000**	**9.041(2.553,32.022)**	**0.001**
ER	0.475(0.216,1.044)	0.064	1.595(0.252,10.084)	0.62
PR	0.481(0.224,1.034)	0.061	0.508(0.085,3.035)	0.458
HER-2	1.003(0.429,2.345)	0.994	1.436(0.462,4.466)	0.532
Ki-67				
Moderate	0.690(0.209,2.273)	0.541	0.382(0.094,1.551)	0.178
High	2.581(0.948,7.022)	0.063	1.298(0.350,4.809)	0.696
P53	1.920(0.827,4.457)	0.129	2.115(0.739,6.050)	0.163
Amount of fibroglandular tissue				
Heterogeneous fibroglandular tissue	0.948(0.414,2.179)	0.899	1.439(0.491,4.215)	0.507
Extreme fibroglandular tissue	1.856(0.630,5.469)	0.262	3.773(0.707,20.154)	0.12
Size(cm)	1.928(0.890,4,176)	0.096	0.921(0.294,2.891)	0.889
Nipple retraction	2.267(0.914,5.621)	0.077	1.299(0.281,5.991)	0.738
Single/multiple	1.158(0.476,2.819)	0.746	1.183(0.336,4.165)	0.793
Lesions	1.057(0.500,2.233)	0.885	0.712(0.256,1.979)	0.514
Mass shape	0.472(0.163,1.365)	0.166	0.624(0.128,3.047)	0.56
Margin	0.224(0.043,1.389)	0.112	0.424(0.032,5.630)	0.516
Boundary				
Obscure	1.469(0.586,3.684)	0.413	1.483(0.439,5.007)	0.526
Shield	1.131(0.436,2.935)	0.800	0.997(0.246,4.043)	0.997
Axillary lymph node enlargement	1.716(0.797,3.694)	0.168	0.909(0.295,2.805)	0.868
E-cad	0.250(0.043,1.452)	0.122		
Location				
Outer lower	0.510(0.054,4.819)	0.557		
Lower inner	1.021(0.314,3.320)	0.973		
Upper inner	1.361(0.434,4.267)	0.597		
Central area	1.531(0.477,4.913)	0.474		
Calcification	1.857(0.601,5.734)	0.166		
Family history	1.927(0.117,31.602)	0.646		
History of giving birth	2.158(0.233,19.947)	0.498		
History of abortion	0.781(0.339,1.799)	0.561		
CA15-3	1.925(0.261,14.179)	0.52		
History of related illness	0.463(0.050,4.284)	0.498		

Table 3. Diagnostic performance

Methods	Sensitivity	Specificity	Accuracy	PPV	NPV
Interstitial edema	19.0(8/42)	95.0(76/80)	68.9(84/122)	66.7(8/12)	69.1(76/110)
Thicken Skin	50.0(21/42)	81.3(65/80)	70.5(86/122)	58.3(21/36)	75.6(65/86)
Subcutaneous fat	19.0(8/42)	83.8(67/80)	61.2(75/122)	38.1(8/21)	66.3(67/101)
connection	14.3(6/42)	98.8(79/80)	69.7(85/122)	85.7(6/7)	68.7(79/115)

Figures

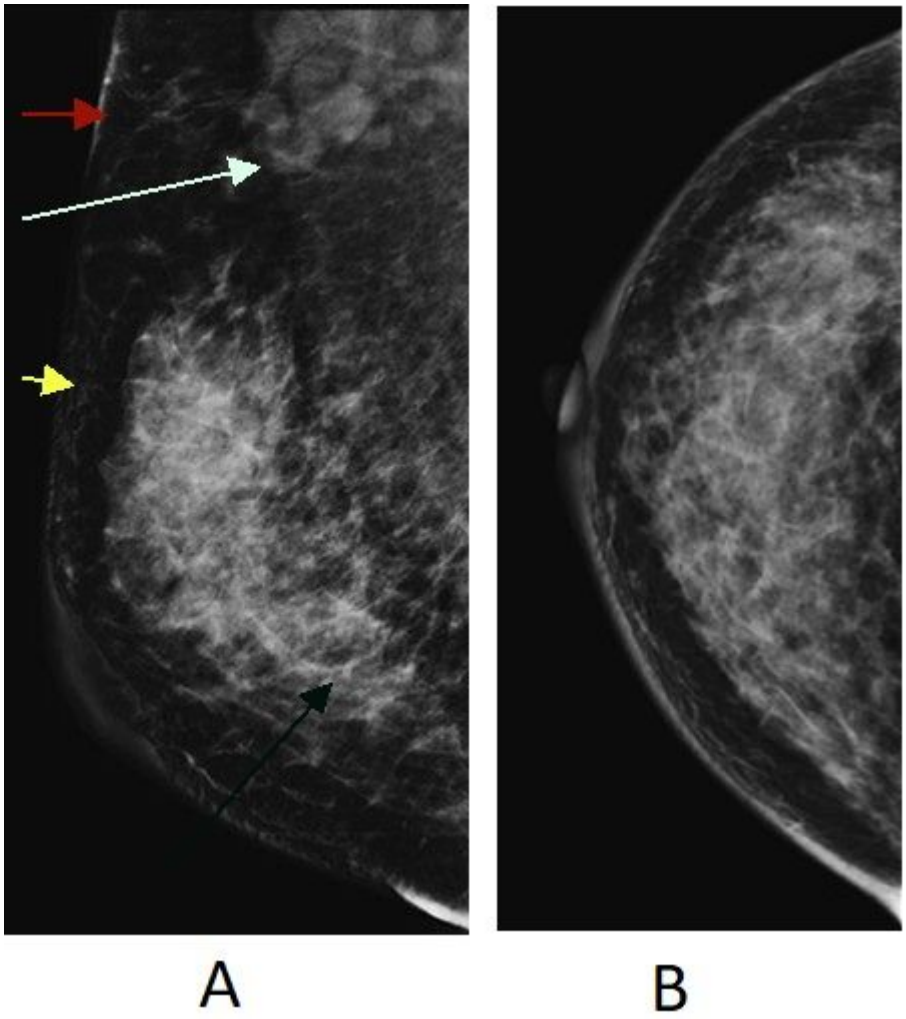

Figure 1

Female, 58 years old, VI positive. The MLO position (Fig. A) and CC position (Fig. B) of digital mammography showed an irregular upper mass with blurred boundaries in the upper outer quadrant of the right breast. Also, interstitial edema(black arrow), blurring of subcutaneous fat layer(yellow arrow), skin thickening(red arrow), and axillary adenopathy(white arrow) were shown in the right breast.

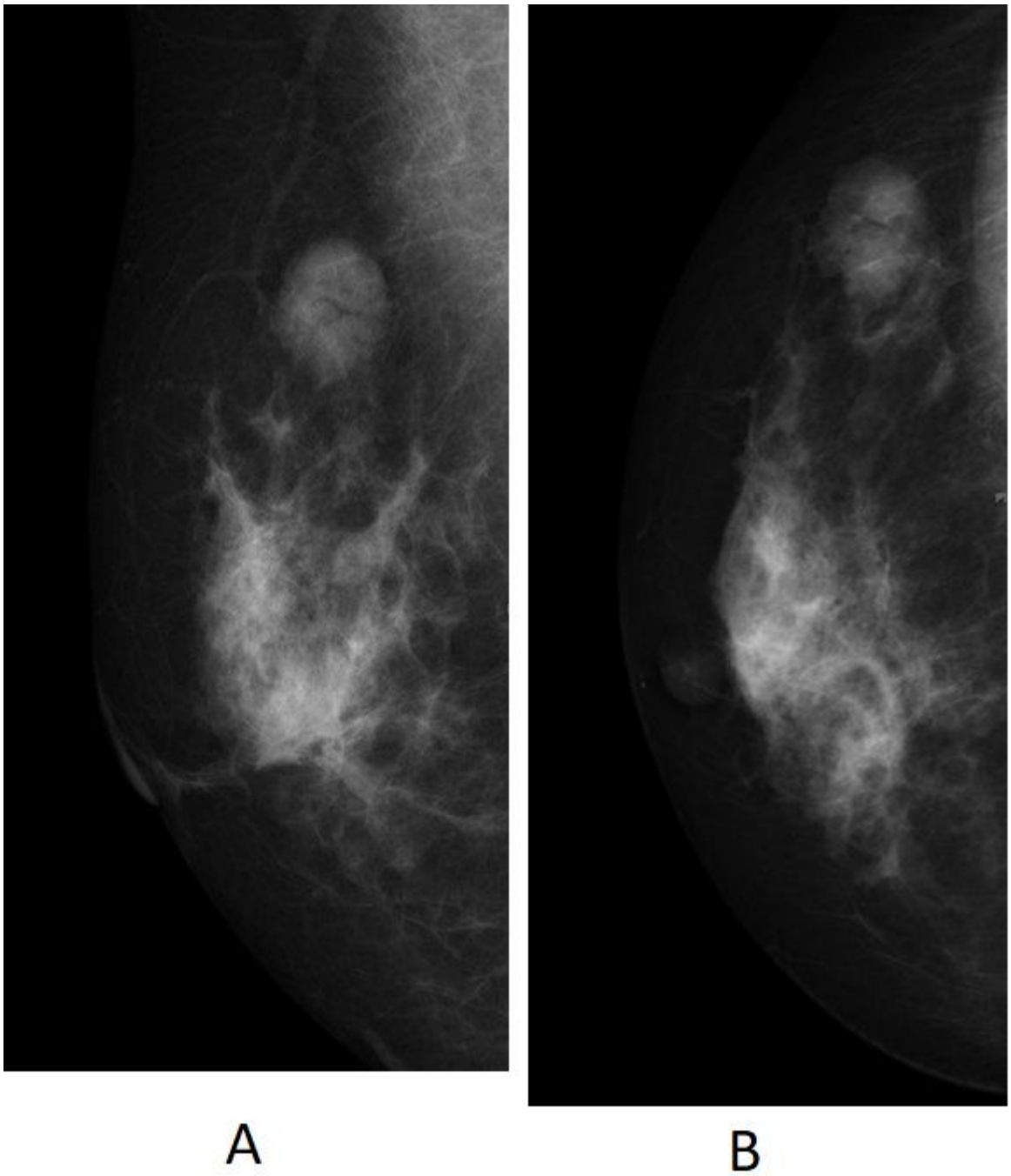

Figure 2

Female, 47 years old, VI negative. The MLO position (Fig. A) and the CC position (Fig. B) of the digital mammography showed a circular mass with smooth edges and clear boundaries in the upper outer quadrant of the right breast, and accompanying patterns such as interstitial edema and skin thickening were not seen.

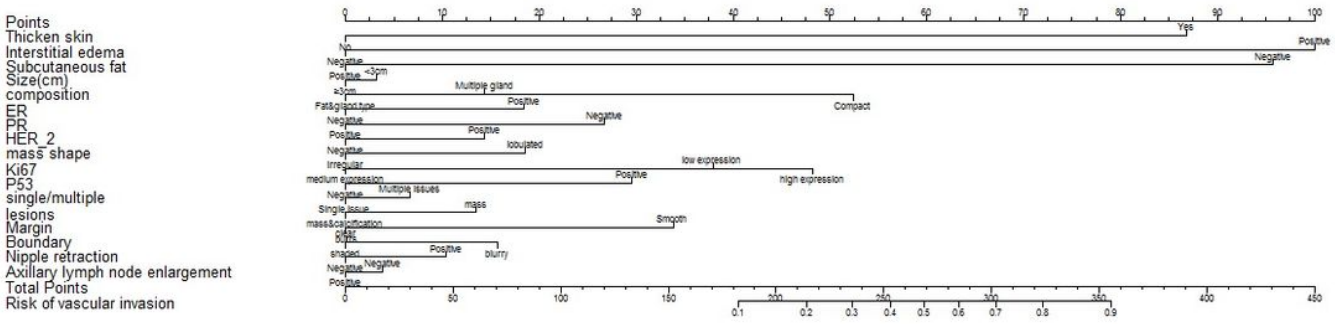

Figure 3

Nomogram of imaging patterns and tumor markers in this study group used for predicting risk of VI occurrence.